Neuropharmacology 116 (2017) 38–49

Contents lists available at ScienceDirect

Neuropharmacology

journal homepage: www.elsevier.com/locate/neuropharm

Diverse arrestin-recruiting and endocytic profiles of tricyclic antipsychotics acting as direct α_{2A} adrenergic receptor ligands

Christopher Cottingham [a, d], Pulin Che [a], Wei Zhang [e], Hongxia Wang [a], Raymond X. Wang [b], Stefanie Percival [a], Tana Birky [a], Lufang Zhou [b], Kai Jiao [c], Qin Wang [a, *]

[a] Department of Cell, Molecular and Developmental Biology, University of Alabama at Birmingham, Birmingham, AL 35294, USA
[b] Department of Medicine, University of Alabama at Birmingham, Birmingham, AL 35294, USA
[c] Department of Genetics, University of Alabama at Birmingham, Birmingham, AL 35294, USA
[d] Department of Biology and Chemistry, Morehead State University, Morehead, KY 40351, USA
[e] Southern Research Institute, Birmingham, AL 35205, USA

ARTICLE INFO

Article history:
Received 8 August 2016
Received in revised form
28 November 2016
Accepted 8 December 2016
Available online 9 December 2016

Keywords:
Antipsychotic
Endocytosis
Arrestin
Biased agonism
α_2 adrenergic receptor
Lipid raft

ABSTRACT

The therapeutic mechanism of action underlying many psychopharmacological agents remains poorly understood, due largely to the extreme molecular promiscuity exhibited by these agents with respect to potential central nervous system targets. Agents of the tricyclic chemical class, including both antidepressants and antipsychotics, exhibit a particularly high degree of molecular promiscuity; therefore, any clarification of how these agents interact with specific central nervous system targets is of great potential significance to the field. Here, we present evidence demonstrating that tricyclic antipsychotics appear to segregate into three distinct groups based upon their molecular interactions with the centrally-important α_{2A} adrenergic receptor (AR). Specifically, while the α_{2A}AR binds all antipsychotics tested with similar affinities, and none of the agents are able to induce classical heterotrimeric G protein-mediated α_{2A}AR signaling, significant differences are observed with respect to arrestin3 recruitment and receptor endocytosis. All antipsychotics tested induce arrestin3 recruitment to the α_{2A}AR, but with differing strengths. Both chlorpromazine and clozapine drive significant α_{2A}AR endocytosis, but via differing clathrin-dependent and lipid raft-dependent pathways, while fluphenazine does not drive a robust response. Intriguingly, *in silico* molecular modeling suggests that each of the three exhibits unique characteristics in interacting with the α_{2A}AR ligand-binding pocket. In addition to establishing these three antipsychotics as novel arrestin-biased ligands at the α_{2A}AR, our findings provide key insights into the molecular actions of these clinically-important agents.

© 2016 Elsevier Ltd. All rights reserved.

1. Introduction

Despite significant progress in our understanding of both G protein-coupled receptor (GPCR) function and the neurobiology of psychiatric disease, psychopharmacology remains frustratingly opaque, fraught with more questions than answers. A major reason for these continued struggles can be found in the fact that many psychopharmacological agents are prototypical “dirty drugs” interacting with numerous molecular targets, including, but not limited to, many GPCRs (Meyer, 2011). The molecular promiscuity of these drugs makes it extremely difficult to develop a coherent working model for their therapeutic mechanisms of action. Progress on this front therefore requires careful investigation of the pharmacological actions these drugs exert at their various binding partners. In the present era of molecular pharmacology, with its explosion in knowledge regarding GPCR structural determination and modeling (Kobilka, 2011; Shoichet and Kobilka, 2012; Costanzi, 2014), such investigation can and should include structural probing in addition to classic *in vitro* and *in vivo* pharmacological techniques.

Psychopharmacological agents belonging to the tricyclic chemical class are particularly noted for their molecular promiscuity (Baldessarini, 2006; Meyer, 2011), and thus represent a particularly

* Corresponding author. 1918 University Boulevard, 986 MCLM, Birmingham, AL 35294, USA.
E-mail address: qinwang@uab.edu (Q. Wang).

http://dx.doi.org/10.1016/j.neuropharm.2016.12.004
0028-3908/© 2016 Elsevier Ltd. All rights reserved.

challenging yet interesting group for study. This class comprises both antidepressant therapeutics used primarily in the pharmacological management of depressive disorders and antipsychotic therapeutics used primarily in the pharmacological management of schizophrenia. In recent years, we have completed extensive studies regarding the tricyclic antidepressant (TCA) compounds, including desipramine (DMI), imipramine, and amitriptyline, with a focus on characterizing novel actions of DMI as a direct ligand at the α_{2A} adrenergic receptor (AR) (Cottingham et al., 2011, 2012a,b, 2014). The α_{2A}AR has long been appreciated as the predominant α_2AR subtype expressed throughout the central nervous system (De Vos et al., 1992; Sastre and García-Sevilla, 1994; Wang et al., 1996), is intimately involved in the function of the brain noradrenergic system, and has been shown to be dysregulated in certain psychiatric disorders (Cottingham and Wang, 2012).

Our previous work has uncovered the novel finding that TCAs function as arrestin-biased ligands at the α_{2A}AR, selectively recruiting the non-visual arrestins (arrestin2/3, also known as β-arrestin1/2) to the α_{2A}AR while not activating any detectable signal transduction through heterotrimeric G proteins (Cottingham et al., 2011, 2014). This arrestin recruitment leads to classical arrestin- and clathrin-mediated GPCR endocytosis with acute exposure. Such arrestin-biased agonism linking to receptor internalization raises the possibility that these compounds could impact the dynamic molecular balance within complex CNS synapses (Molinoff, 2011) by initiating endocytosis and altering the cell-surface availability (von Zastrow and Williams, 2012; Irannejad et al., 2015) of α_{2A}ARs. Although arrestin-biased agonism of GPCRs generally has been established in the field for many years now (Violin and Lefkowitz, 2007; Rajagopal et al., 2010), our work provided the first evidence for this phenomenon at the α_{2A}AR specifically. Currently, it is unclear whether any of the tricyclic antipsychotics share the properties of the TCAs as direct arrestin-biased α_{2A}AR ligands. In the present study, we have therefore set out to characterize representative tricyclic antipsychotic compounds as direct α_{2A}AR ligands. Our data indicate that, while all tricyclics studied can interact with the α_{2A}AR at physiologically-relevant affinity values, these compounds exhibit widely varying functional profiles as α_{2A}AR ligands, especially with respect to arrestin3 (Arr3) recruitment and the induction of receptor endocytosis. Additionally, *in silico* molecular modeling suggests that differences exist in how the compounds studied interact with the α_{2A}AR ligand-binding site. These findings are of great value, as they highlight the mechanistic differences between chemically-similar antidepressants and antipsychotics, and have the potential to inform the development of next-generation agents with improved pharmacological precision.

2. Materials & methods

2.1. Drugs

All pharmacological agents, with the exception of clozapine, were purchased from Sigma-Aldrich. These agents were supplied in the following forms: chlorpromazine HCl, fluphenazine diHCl, norepinephrine (NE) bitartrate salt, prazosin HCl, propranolol HCl. Clozapine was obtained from the National Institute of Mental Health Chemical Synthesis and Drug Supply Program, supplied in an unmodified chemical form. Concentrated stock solutions of all agents were prepared by dissolving in water, with the exception of clozapine, which was initially dissolved in DMSO before dilution in water.

2.2. Cell culture

Heterologous cell lines stably expressing an N-terminal hemagglutinin (HA) epitope-tagged murine α_{2A}AR were used for all experiments. The generation and characterization of the HEK 293 (Schramm and Limbird, 1999) and both the wild-type (WT) and arrestin-null (Arr2,3$^{-/-}$) mouse embryonic fibroblast (MEF) stable cell lines (Brady et al., 2005; Cottingham et al., 2011) has been described previously. The HEK 293 line expresses HA-α_{2A}ARs at a density of 7–8 pmol/mg (Schramm and Limbird, 1999), while the MEF lines express HA-α_{2A}ARs at a density of 400 fmol/mg (Cottingham et al., 2011). All three cell lines were cultured in Dulbecco's modified Eagle medium (DMEM, Life Technologies) supplemented with 10% fetal bovine serum (Atlanta Biologicals) and 1% penicillin/streptomycin (Life Technologies), and maintained at 37 °C in a humidified 5% CO_2 incubator.

2.3. Radioligand binding

Binding of the various drugs to the α_{2A}AR was assessed by competition for binding with a ^{3}H-labeled α_2AR antagonist ([^{3}H] RX821002, PerkinElmer). All radioligand binding experiments were done in crude membrane preparations from the stable HEK 293 cell line, and in the presence of Gpp(NH)p to eliminate binding regulation by heterotrimeric G proteins, as previously described (MacMillan et al., 1996; Lu et al., 2009; Cottingham et al., 2011). Determination of orthosteric site binding was performed according to a method described by Limbird (2005) and utilized in our previous study on DMI (Cottingham et al., 2011). Concentration-response curves were constructed and K_i values determined by GraphPad Prism software (GraphPad Software, San Diego, CA). Software-determined K_i values were confirmed by hand calculation according to the method of Cheng and Prusoff/Chou (Cheng and Prusoff, 1973; Chou, 1974), utilizing the equation $K_i = IC_{50}/[1 + ([\text{radioligand}]/K_i \text{ radioligand})$. Saturation binding was performed to assess receptor density following prolonged treatments with various ligands as we have described previously (Lu et al., 2009; Cottingham et al., 2011). Raw radioligand binding values were normalized to total protein content in each reaction.

2.4. [^{35}S]GTPγS binding

Ligand-stimulated coupling of heterotrimeric G proteins to the α_{2A}AR was assessed by measuring [^{35}S]GTPγS binding to crude membrane preparations from the stable HEK 293 cell line as previously described (Tan et al., 2002; Cottingham et al., 2011). [^{35}S] GTPγS (PerkinElmer) was used at a concentration of 320 pM (1250 Ci/mmol) per reaction tube. Ligand-stimulated G protein coupling was calculated as a fold increase in binding over no-ligand control reactions.

2.5. Western blot

The WT MEF cell line with stable HA-α_{2A}AR expression described above was utilized to assess clozapine-stimulated α_{2A}AR-mediated activation of the ERK1/2 MAP kinase pathway via Western blot targeting phospho-ERK1/2 (pERK1/2). Western blot was carried out as previously described (Cottingham et al., 2011; Cottingham et al., 2012a,b). Primary antibodies were phospho-p44/42 MAPK (ERK1/2, Thr202/Tyr204) mouse mAb (Cell Signaling), total p44/42 MAPK (ERK1/2) rabbit polyclonal (Cell Signaling), with HRP-conjugated anti-mouse and anti-rabbit IgGs obtained from Millipore. Membranes were first probed for phospho-ERK1/2, then stripped and re-probed for total ERK1/2.

2.6. FLIM-FRET

Fluorescence lifetime imaging microscopy (FLIM) was the

technique used to observe α_{2A}AR/Arr3 interaction in the form of FRET. Our method for performing FLIM-FRET to detect interaction between CFP-tagged α_{2A}ARs and YFP-tagged Arr3, as well as the generation of CFP-α_{2A}AR and YFP-Arr3 constructs, has been described previously in detail (Cottingham et al., 2011). Briefly, parental HEK 293 cells were transiently transfected with the CFP-α_{2A}AR plasmid alone or in combination with the YFP-Arr3 plasmid using Lipofectamine 2000 (Sigma), according to the manufacturer instructions. After transfection, live cells plated onto 8-well microslides (ibidi GmbH) were subjected to one-photon (confocal) FLIM imaging using a Becker and Hickl Simple Tau Time Correlated Single Photon Counting Module and pulsed diode 405 nm laser (Becker and Hickl GmbH) in conjunction with a Zeiss LSM 710 confocal microscope. SPCImage software (Becker and Hickl GmbH) was then used to analyze the resulting FLIM images, returning a CFP fluorescent lifetime value for each cell imaged. Cell-surface points were selected for these CFP lifetime analyses, with basic confocal images of each cell used to confirm the location. For each data set shown in Fig. 4B, C, 5 and 6 individual cells from 2 to 3 different transfected samples were subjected to FLIM, with a raw CFP lifetime value (in picoseconds) obtained. These raw lifetime values (t_{CFP} for CFP-only cells and t_{FRET} for CFP/YFP-expressing cells) were then used to calculate FLIM-FRET efficiency (E) values, according to the formula $E = 1 - (t_{FRET}/t_{CFP})$.

2.7. Intact cell-surface ELISA

Ligand-stimulated α_{2A}AR endocytosis was assessed quantitatively in MEF cells using a previously described method (Brady et al., 2003; Xu et al., 2008; Cottingham et al., 2011) for intact cell-surface ELISA. MEF cells were seeded onto 96-well culture plates at a density of 1×10^4 cells/well, the primary anti-HA antibody (HA11, mouse monoclonal, Covance) was used at a final dilution of 1:3000, and the secondary antibody (anti-mouse HRP-conjugated IgG, Millipore) was used at a final dilution of 1:2000. Endocytosis was measured as a percent decrease in cell-surface density from no-ligand control wells.

2.8. cAMP assay

cAMP assays were performed using the AlphaScreen® Assay Kit (PerkinElmer) as previously described (Chen et al., 2012). Briefly, cultured HEK 293 cells stably expressing the α_{2A}AR (Tan et al., 2002; Cottingham et al., 2011) were resuspended with the stimulation buffer (1× HBSS, 0.1% BSA, 0.5 mM IBMX, 5 mM HEPES, pH 7.4) and mixed with anti-cAMP acceptor beads. The mix was divided into 3 groups and incubated at 37 °C with the following chemicals: (1) vehicle; (2) 10 μM forskolin (Sigma); (3) 10 μM forskolin and ligand of interest. After a 20-min treatment, biotinylated cAMP/streptavidin donor beads (in 0.1% BSA, 0.3% Tween-20, 5 mM HEPES, pH 7.4) were added to the mix and incubated for an additional 30 min at room temperature. Fluorescence intensity was then analyzed on a Biotek Synergy2 plate reader.

2.9. Immunofluorescent staining

Ligand-stimulated α_{2A}AR endocytosis was assessed qualitatively in MEF cells using a primary antibody pre-labeling method for staining of HA-α_{2A}ARs that has been well-described previously (Xu et al., 2008; Lu et al., 2009). MEF cells were seeded onto glass cover slips in 24-well culture plates at a density of 2×10^4 cells/well. Surface α_{2A}ARs were pre-labeled with HA11 (1:125 dilution) prior to stimulation, with secondary antibody (Alexa488-conjugated anti-mouse IgG, Molecular Probes) used at a 1:1000 dilution to detect pre-labeled receptors after stimulation. Stained cells were visualized by confocal microscopy on a Zeiss LSM 710 (Carl Zeiss) or a Nikon A1 confocal microscope. Confocal images were analyzed using imaging software NIS-Elements AR4.13.00. The degree of colocalization between two proteins was quantified by Pearson's correlation coefficient using NIS-Elements AR4.13.00 subprogram Analysis Control-Colocalization.

2.10. K^+ and cholesterol depletion protocols

A K^+ depletion protocol for blocking formation of clathrin-coated pits was performed as previously described on the ArrWT MEF cell line (Cottingham et al., 2011). This method was used in conjunction with intact cell-surface ELISA to determine the clathrin-dependence of ligand-stimulated α_{2A}AR endocytosis. Control cells received a sham treatment to allow for direct comparison with K^+-depleted cells. Control and K^+-depleted cells were analyzed via intact cell-surface ELISA (see above) in parallel, on the same 96-well plate.

Cholesterol depletion was achieved by treatment of cells with methyl-β-cyclodextrin (MβCD, Sigma-Aldrich). Specifically, cells were pre-treated with 10 mM MβCD (diluted to the final concentration in serum-free DMEM) for 30 min at 37 °C prior to a trafficking experiment; 10 mM MβCD was then maintained throughout the experiment. Control cells simply received serum-free DMEM instead; both control and MβCD-treated cells were analyzed in parallel for each experiment via intact cell-surface ELISA or immunofluorescent staining (see above).

2.11. Molecular modeling

Structural model generation and molecular docking studies were conducted using the programs of the Schrödinger Suite 2014 (Schrödinger, LLC, New York, NY). A human α_{2A}AR homology model was built based on the crystal structure of the β_2AR (PDB ID: 3PDS) using the *Prime* program (Prime, version 1.6, 2007). The 3D structures of ligands were prepared using the *LigPrep* program (LigPrep, version 2.3, 2009). The *Glide* program (Glide, version 6.3, 2014) was used for docking studies. Specifically, the Induced-Fit-Docking (IFD) protocol (Sherman et al., 2006), which is capable of sampling dramatic side-chain conformational changes as well as minor changes in protein backbone structure, was applied to explore the binding mode of despiramine, chlorpromazine, clozapine and fluphenazine. NE was also docked as a control for comparison. Compounds were docked into the substrate binding site of the α_{2A}AR structural model. Residues within 5 Å of the docked compound were allowed to be flexible and the docked results were scored using the extra-precision (XP) mode of *Glide*. The best scored binding pose of each compound was select for the comparison of protein-ligand interactions. Residue numbers were based on Ballesteros Weinstein sequencing (Ballesteros and Weinstein, 1995).

2.12. Software & statistical analysis

Representative chemical structures for the tricyclic agents were prepared using ChemDraw software (CambridgeSoft). Dose response curves and other graphs were constructed using GraphPad Prism (GraphPad Software), which was also used to calculate K_i values and perform statistical tests.

3. Results

3.1. Tricyclic antipsychotic compounds bind to the α_{2A}AR at the orthosteric site

Three representative members of the tricyclic antipsychotic

chemical class were selected for characterization as α_{2A}AR ligands: chlorpromazine, clozapine, and fluphenazine. Of those selected, two (chlorpromazine and fluphenazine) are typical, or first-generation, antipsychotics, while one (clozapine) is an atypical, or second-generation, antipsychotic (Meyer, 2011). All of these compounds share a common tricyclic core structure with a characteristic long side chain (or fragment) arising from the central ring; the compounds vary slightly in central ring structure and small substituent identity, and radically in the nature of the characteristic long side chain (Fig. 1A). Our first goal was to utilize competition radioligand binding analysis to determine accurate affinity (K_i) values for the selected antipsychotics at the murine HA-α_{2A}AR in membrane preparations from our HEK 293 cell line with stable expression of the receptor. Although initial results indicated that the antipsychotics were competing with the radiolabeled α_2AR antagonist for binding to the same orthosteric binding site on the

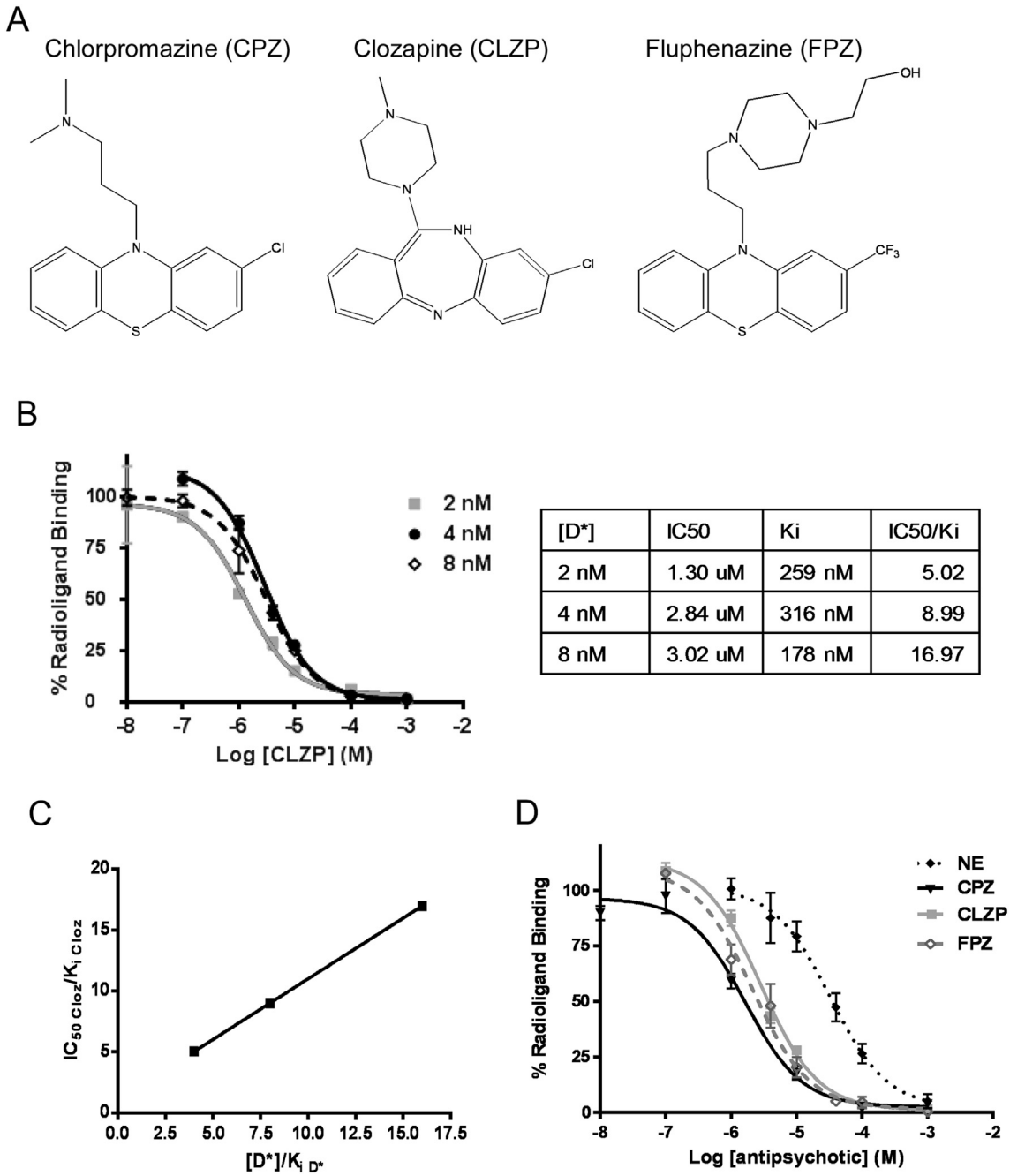

[D*]	IC50	Ki	IC50/Ki
2 nM	1.30 uM	259 nM	5.02
4 nM	2.84 uM	316 nM	8.99
8 nM	3.02 uM	178 nM	16.97

Fig. 1. The tricyclic antipsychotic compounds show orthostatic binding to the α_{2A}AR. (A) Chemical structures of the tricyclic antipsychotic compounds tested in this study. (B) Competition binding curves for clozapine (CLZP) at the α_{2A}AR conducted at varying concentrations ([D*]) of radioligand ([^{3}H]RX821002), and the corresponding IC_{50} and K_i values for CLZP obtained from analysis of those curves. (C) The IC_{50}:K_i values obtained in panel B were plotted as a function of radioligand concentration ([D*], normalized to its own Ki at the α_{2A}AR), according to the method described by Limbird (2005) for analyzing orthosteric binding to a GPCR. Linear regression analysis returned an R^2 value of 1.000, demonstrating the strong positive correlation indicative of binding to the orthosteric site. (D) Comparison of competition binding curves obtained for the three tricyclic antipsychotic compounds tested in this study and the endogenous α_{2A}AR agonist NE; these curves were constructed using a consistent radioligand concentration of 4 nM. Data are mean ± S.E. and represent n = 3–4. CPZ, chlorpromazine; CLZP, clozapine; FPZ, fluphenazine.

α_{2A}AR, it is possible for ligand binding to an allosteric site to appear competitive in this assay. We have previously reported that TCAs do in fact bind to the α_{2A}AR orthosteric site (Cottingham et al., 2011), applying a method described by Limbird (2005) which requires the construction of competition binding curves at differing concentrations of radioligand. Here, we applied the same method for clozapine in order to confirm that the tricyclic antipsychotics are also capable of binding the orthosteric site. We obtained IC_{50} to K_i value ratios for clozapine from competition binding curves constructed at radioligand concentrations of 2, 4, and 8 nM (Fig. 1B). As shown in Fig. 1C, plotting these ratios as a function of radioligand concentration (normalized to its own K_i) revealed a strong linear relationship, characteristic of binding that is truly competitive with the radioligand at the receptor orthosteric site.

In concordance, typical sigmoidal concentration-response curves were able to be constructed for chlorpromazine, clozapine, and fluphenazine (Fig. 1D). K_i values obtained from analysis of these curves are shown in Table 1. As a group, the tricyclic antipsychotics bind the α_{2A}AR with stronger affinity than the TCAs (Cottingham et al., 2011, 2014). To provide physiological context, Table 1 also includes reported average clinical blood plasma levels for these drugs. By comparing our experimentally-determined K_i values with the clinically-relevant therapeutic levels (Baldessarini and Tarazi, 2006), it becomes apparent that the affinity values for each of the tricyclic compounds are either well within or extremely close to the relevant therapeutic ranges. Furthermore, as also shown in Table 1, our experimentally-determined K_i values for the murine α_{2A}AR are quite similar to those that have been reported in the literature for the human α_{2A}AR (NIMH Psychoactive Drug Screening Program K_i Database).

3.2. Tricyclic antipsychotic compounds do not activate G protein signaling but can drive arrestin3 recruitment to the receptor

Having confirmed the high-affinity binding of our selected antipsychotics to the α_{2A}AR, the logical next step was to determine whether any of these compounds were capable of stimulating α_{2A}AR coupling to heterotrimeric G proteins. Using membrane preparations from our HEK 293 cell line with stable expression of the receptor, we performed the classic pharmacological technique of [^{35}S]GTPγS binding. We found that none of the antipsychotic compounds were able to drive any significant [^{35}S]GTPγS binding compared with the no-ligand control; the endogenous AR agonist norepinephrine (NE) was evaluated in parallel as a positive control (Fig. 2A). Note that NE stimulation was done in the presence of 1 μM prazosin and propranolol, to block any potential NE-induced G protein coupling to $\alpha_1/\alpha_{2B}/\alpha_{2C}$ and β ARs, respectively. Consistent with their inability to induce G protein coupling, none of the antipsychotic compounds could drive the canonical $G\alpha_i$-mediated inhibition of cAMP production, while NE, when evaluated in parallel, caused a nearly 50% inhibition of cAMP production (Fig. 2B). As an additional measure, we elected to evaluate our selected antipsychotics for potential activation of an additional

Table 1
Summary of pharmacological analysis of tricyclic antipsychotics. Therapeutic ranges are as reported in Baldessarini and Tarazi (2006). Values for the human α_{2A}AR are as reported in the NIMH Psychoactive Drug Screening Program (PDSP) K_i Database.

Parameter	Clozapine	Chlorpromazine	Fluphenazine
IC_{50} (μM)	2.84	1.66	2.10
K_i (nM)	316	185	234
Therapeutic range			
ng/ml	300–500	>30–750	20–100
nM	920–1530	90–2350	50–230
Reported values at human α_{2A}AR (nM)			
Range	24–142	78–558	314
Avg.	89.5	251	314

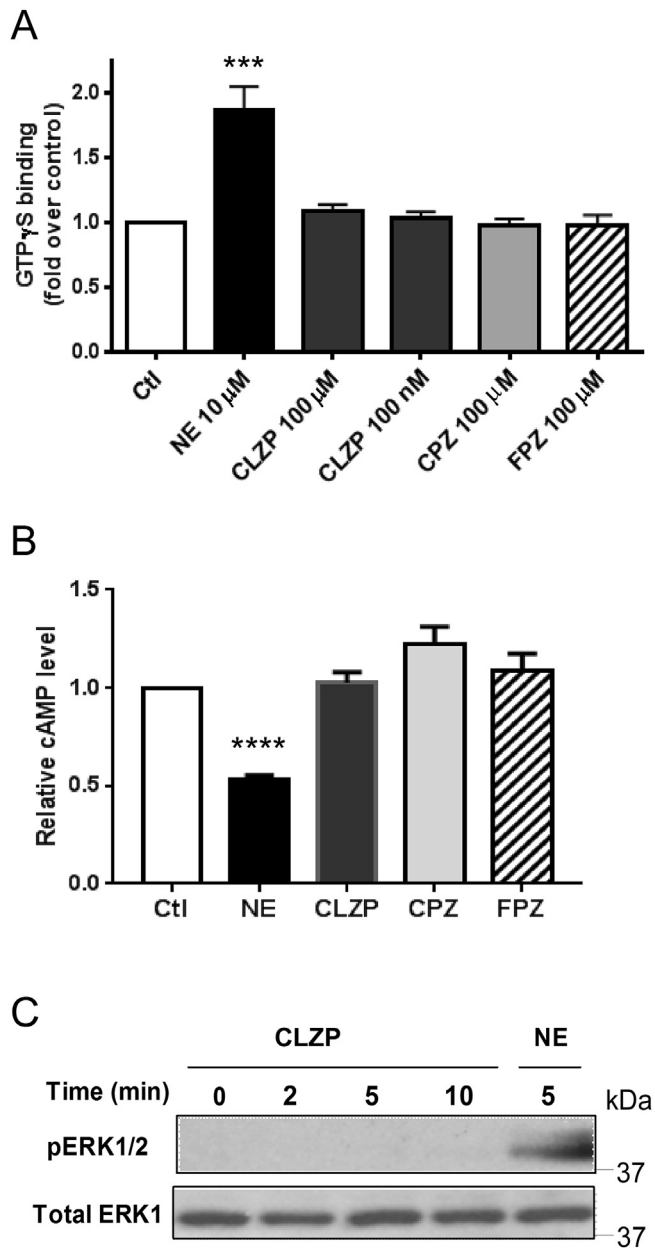

Fig. 2. Binding of the tricyclic antipsychotic compounds to the α_{2A}AR does not lead to activation of G protein-mediated signaling. (A) [^{35}S]GTPγS binding was conducted as described in Materials & Methods in order to assess ligand-stimulated activation of heterotrimeric G proteins by α_{2A}ARs. The crude membrane preparations were exposed to either a tricyclic antipsychotic compound or the endogenous α_{2A}AR agonist NE at the concentration indicated for each data set. An internal non-stimulated control (Ctl) for each experiment was set as 1.0-fold. Data are mean ± S.E. and represent n = 4–6. ***, $p < 0.001$, NE versus control by unpaired Student's *t*-test. (B) cAMP assays with cells stimulated by different ligands at 10 μM. NE was used as a positive control for α_{2A}AR-mediated inhibition of cAMP production. The cAMP level with forskolin stimulation alone (Ctl) for each experiment was set as 1.0 fold. Data are mean ± S.E. and represent n = 6–10. ****, $p < 0.0001$, NE versus forskolin alone control by paired Student's *t*-test. (C) Western blot to assay for activation of the downstream α_{2A}AR effector ERK1/2 MAP kinase; accumulation of phospho-ERK1/2 (pERK1/2) indicates activation of the signaling cascade. Cells were stimulated with clozapine (1 μM) for the indicated times; the endogenous α_{2A}AR agonist NE (10 μM, 5 min stimulation) was used as a positive control for α_{2A}AR activation. A blot image representative of n = 3 independent experiments is shown.

downstream effector, specifically the ERK1/2 MAP kinase cascade. Although many GPCRs elicit ERK activation through arrestins, this cascade is well-established as a readout for classical, G protein dependent signal transduction in response to α_{2A}AR activation by agonists (Wang et al., 2004, 2006). As shown in Fig. 2C, we were unable to detect any ERK1/2 activation in response to clozapine. Taken together, our data obtained using multiple independent approaches suggest that the tricyclic antipsychotic compounds tested in this study do not activate G protein-mediated signaling.

Given our past finding that the TCA DMI is an arrestin-biased ligand at the α_{2A}AR, selectively driving Arr3 recruitment to the receptor in the absence of any G protein coupling, we proceeded to evaluate whether any of our G protein-neutral antipsychotics were able to stimulate recruitment of Arr3 to the α_{2A}AR. Our previously established FLIM-FRET technique allowed us to assess Arr3 recruitment to cell-surface α_{2A}ARs in live cells following exposure to the selected tricyclic antipsychotics. In these experiments, interaction between CFP-tagged α_{2A}AR and YFP-tagged Arr3 will result in FRET, detectable as a decrease in the fluorescence lifetime of the CFP donor which results from energy transfer to YFP. As described above, these lifetime values are used to calculate FLIM-FRET efficiency (E); increasing E values represent increasing α_{2A}AR/Arr3 interaction. In Fig. 3A, we have provided a set of representative images to illustrate the expression and distribution of the recombinant CFP-α_{2A}AR and YFP-Arr3 proteins in the live HEK 293 cells. Importantly, these images also demonstrate that CFP-α_{2A}ARs are being delivered to the cell surface. FLIM-FRET analysis of the tricyclic antipsychotics revealed that chlorpromazine and fluphenazine drive robust α_{2A}AR/Arr3 interaction, while clozapine drives a comparatively weaker, though still significant, α_{2A}AR/Arr3 interaction (Fig. 3B). Collectively, the data presented thus far suggest that our selected tricyclic antipsychotics share the property of arrestin-biased α_{2A}AR agonism with the previously-evaluated TCAs.

3.3. The tricyclic antipsychotic compounds have variable capacity to drive α_{2A}AR endocytosis

Our observation of antipsychotic-induced Arr3 recruitment, along with our previous data on TCAs (Cottingham et al., 2011, 2014), led us to next investigate whether acute exposure to the antipsychotics can induce α_{2A}AR endocytosis. As shown in Fig. 4A, immunostaining assays revealed that both chlorpromazine and clozapine drive robust α_{2A}AR endocytosis, indicated by the appearance of characteristic intracellular punctae containing endocytosed receptors, which were pre-labeled prior to stimulation. We further confirmed the endocytic response using cell-surface ELISA, a technique which also allowed us to quantify endocytosis by detected cell surface receptor amount following stimulation. As shown in Fig. 4B, clozapine and chlorpromazine caused approximately 40% and 30% receptor loss from the cell surface, respectively. Interestingly, although fluphenazine was found to induce α_{2A}AR/Arr3 interaction, and with a strength similar to chlorpromazine (Fig. 3B), unlike chlorpromazine, it failed to induce detectable endocytosis of the receptor (Fig. 4A and B). These data indicate that our selected antipsychotics possess differential capacities to drive α_{2A}AR endocytosis, and, given the comparatively weak Arr3 recruitment capacity of clozapine (Fig. 3B), raise additional questions about the mechanism underlying the observed receptor endocytosis.

To address these questions, we further tested the ability of clozapine and chlorpromazine to drive α_{2A}AR endocytosis in arrestin-null (Arr2,3$^{-/-}$) MEF cells. The α_{2A}AR endocytic response to chlorpromazine was lost in the arrestin-null cells (Fig. 5A), while the response to clozapine was preserved (Fig. 5B). This finding

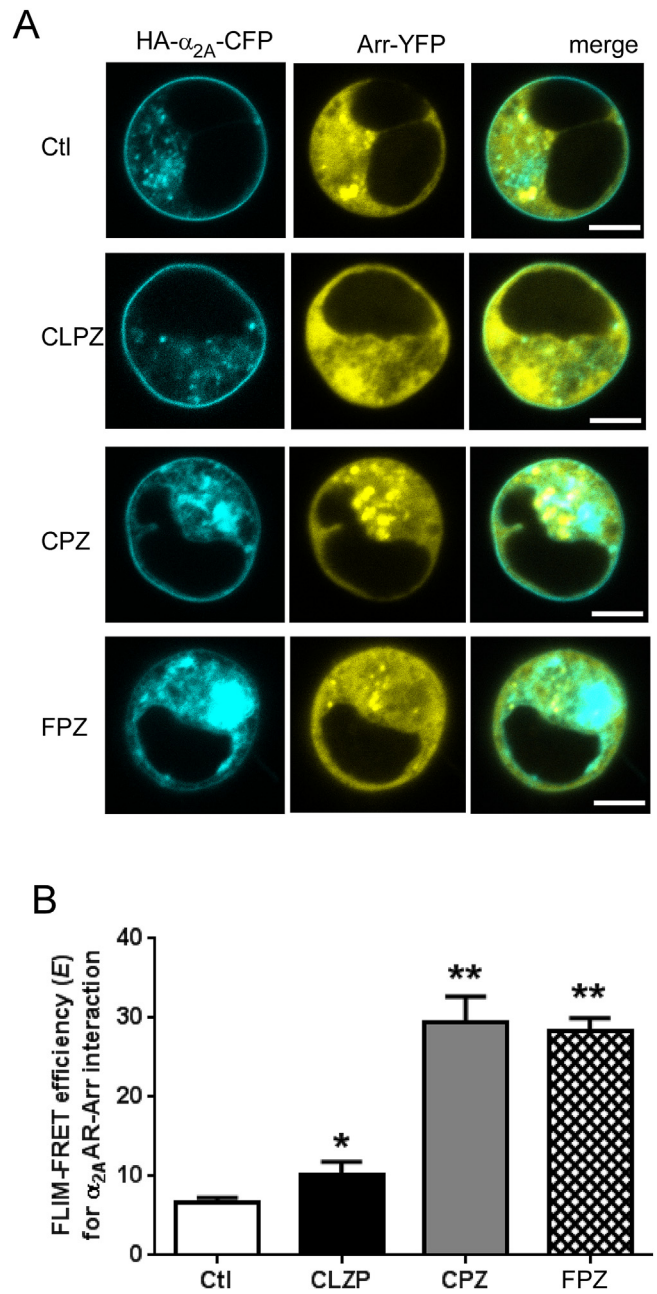

Fig. 3. Differential arrestin3 recruitment to the α_{2A}AR by tricyclic antipsychotic compounds. (A) Representative confocal images of HEK 293 cells transiently transfected with the recombinant CFP-α_{2A}AR and YFP-Arr3 constructs and stimulated with different ligands. (B) FLIM-FRET efficiency (E) values were obtained as described in Materials & Methods. Cells expressing both CFP-α_{2A}AR and YFP-Arr3 were analyzed in either the absence (Ctl) or presence of the indicated tricyclic antipsychotic compound at a concentration of 1 μM. Data are mean ± S.E. and represent n = 6–7. *, $p < 0.05$ versus Ctl; **, $p < 0.01$ versus Ctl by unpaired Student's t-test. CPZ, chlorpromazine; CLZP, clozapine; FPZ, fluphenazine.

indicates that chlorpromazine-induced α_{2A}AR endocytosis is arrestin-dependent, while clozapine-induced α_{2A}AR endocytosis is arrestin-independent. In an attempt to further clarify the mechanism underlying clozapine-driven α_{2A}AR endocytosis, we used chemical approaches to disrupt other potential endocytic machinery components. First, we utilized a K^+ depletion method, which has been demonstrated to disrupt the formation of clathrin-coated pits at the plasma membrane (Hansen et al., 1993). This

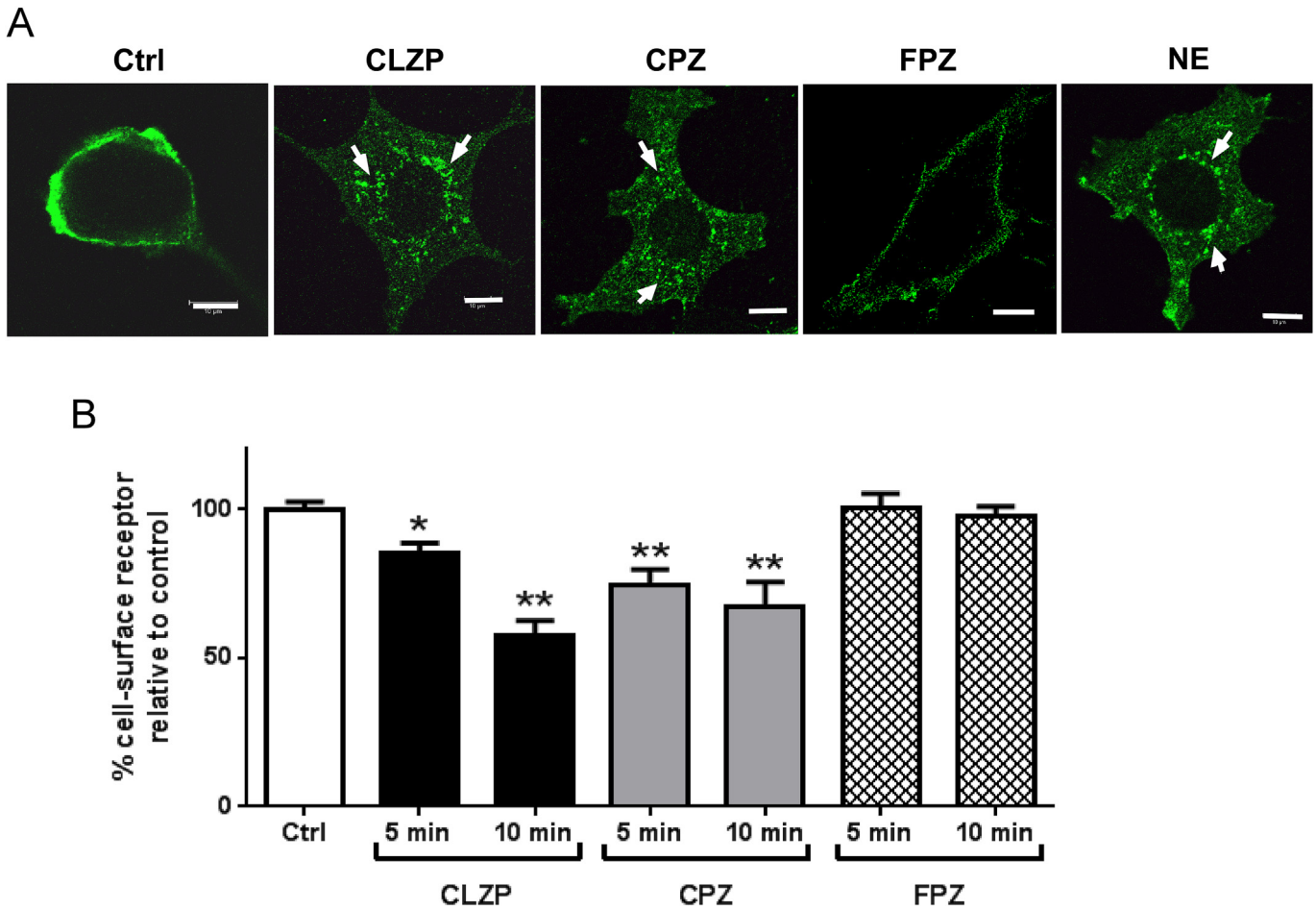

Fig. 4. Tricyclic antipsychotic compounds exhibit varying abilities to induce α_{2A}AR endocytosis. (A) Immunostaining reveals ligand-stimulated α_{2A}AR endocytosis, indicated by the appearance of characteristic intracellular punctae (arrows) containing endocytosed pre-labeled receptors. Cells were stimulated for 30 min with the indicated drugs at a concentration of 1 μM (CLZP, CPZ and FPZ) or 10 μM (NE). Confocal images shown are representative of n = 3 independent experiments. (B) Quantitative analysis of ligand-stimulated α_{2A}AR endocytosis via intact cell surface ELISA. Cells were stimulated with antipsychotics (1 μM) as indicated prior to ELISA. Data for stimulated cells are expressed as a percentage of an internal non-stimulated control (Ctl), which is set as 100% cell-surface receptor. Data are mean ± S.E. and represent n ≥ 5 independent replicates. *, $p < 0.01$ versus Ctl; **, $p < 0.001$ versus Ctl by unpaired Student's *t*-test.

manipulation failed to prevent clozapine-driven α_{2A}AR endocytosis (Fig. 5C). Collectively, our data indicate that clozapine binding to α_{2A}ARs does not engage the canonical arrestin- and clathrin-mediated pathway for GPCR endocytosis.

In addition to the relatively more common canonical pathway through clathrin-coated pits (Tan et al., 2004; Hanyaloglu and von Zastrow, 2008), GPCRs can alternatively internalize through lipid rafts (Chini and Parenti, 2004; Barnett-Norris et al., 2005; Allen et al., 2007). Therefore, we next tested whether disruption of lipid rafts by MβCD treatment could block clozapine-induced internalization of α_{2A}ARs. In cells treated cells with MβCD, internalization induced by clozapine stimulation was completely abolished, as revealed by immunostaining with receptor pre-labeling (Fig. 6A and B). Meanwhile, internalization of α_{2A}AR induced by NE, which occurs through an arrestin- and clathrin-dependent pathway (Cottingham et al., 2011), was not affected by MβCD treatment (Fig. 6C and D). Blockade of clozapine-induced internalization by MβCD was also demonstrated by cell-surface ELISA method (Fig. 6E).

We further examined colocalization of the receptor and caveolin-1 before and after clozapine stimulation. In the naïve state, there is a significant portion of α_{2A}ARs localized in caveolin-rich domains of the plasma membrane (Fig. 7A and B). Following clozapine stimulation, colocalized α_{2A}AR and caveolin was found within the cytoplasm (Fig. 7A and B). Taken together, these data suggest that the clozapine-bound α_{2A}ARs internalize through caveolae-mediated endocytosis.

3.4. *The tricyclic antipsychotic compounds display differential docking to the α_{2A}AR ligand-binding site in silico*

To explore structural insights regarding the observed biochemical profiles of the tricyclic compounds, we conducted *in silico* molecular docking studies using a constructed α_{2A}AR homology model. The three antipsychotic compounds under evaluation in the present study were evaluate alongside the TCA DMI, which was the major subject of our previously published work. While all four tricyclic compounds docked well into the ligand-binding site, which is mainly formed by residues from transmembrane domain (TM) 3 (TM3), TM5, TM6, TM7 and the extracellular loop 2 (xl2) of α_{2A}AR, there are clear differences among their predicted binding modes (Fig. 8). Each of the four compounds has a similar tricyclic core structure, but with a very different fragment (i.e., the characteristic long side chain) attached to it; the

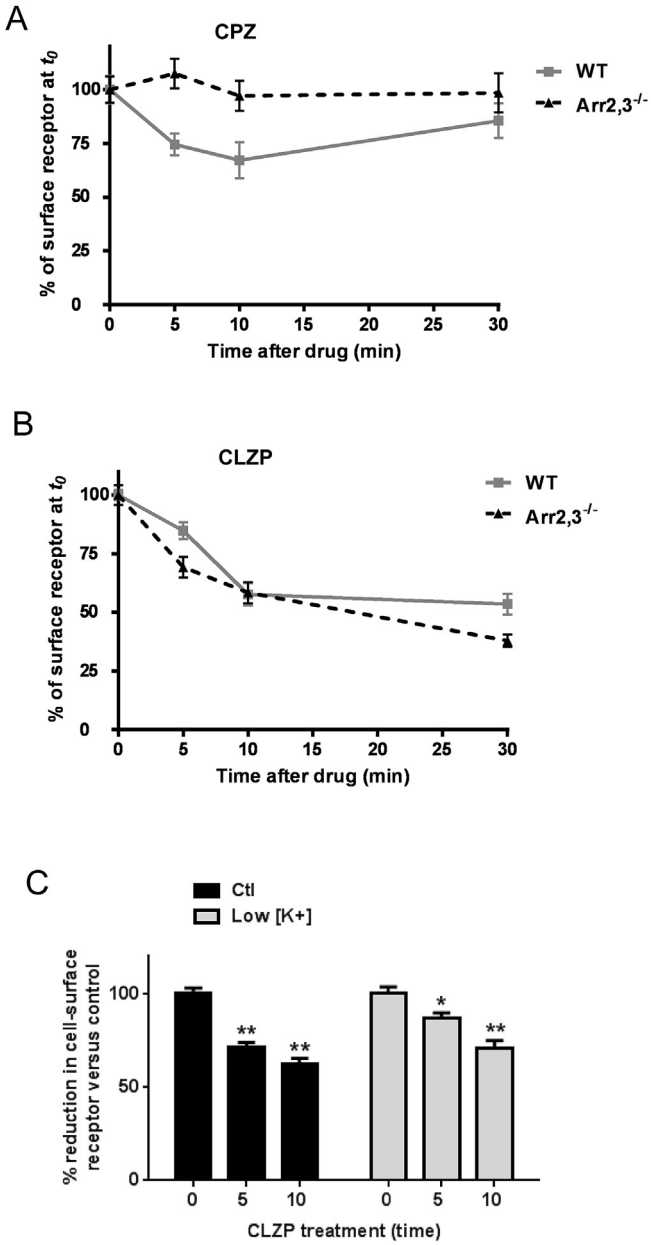

Fig. 5. Chlorpromazine-induced α_{2A}AR endocytosis occurs via an arrestin-dependent mechanism while clozapine-induced α_{2A}AR endocytosis is arrestin- and clathrin-independent. (A) Quantitative analysis of chlorpromazine-stimulated α_{2A}AR endocytosis via intact cell surface ELISA in WT and arrestin-null (Arr2,3$^{-/-}$) cells. Cells were stimulated with chlorpromazine (CPZ) (1 μM) for 5, 10, and 30 min; endocytosis is indicated by a reduction in cell-surface receptor versus an internal non-stimulated control (here, t = 0), which is set as 100% cell-surface receptor. Data are mean ± S.E. and represent n ≥ 13 independent replicates. (B) The same quantitative analysis as in panel A, but substituting clozapine (CLZP) for chlorpromazine. Data are mean ± S.E. and represent n ≥ 13 independent replicates. (C) To assess the clathrin-dependence of ligand-stimulated α_{2A}AR endocytosis, cells were subjected to the K^+-depletion protocol described in Materials & Methods for disrupting clathrin-coated pit formation prior to stimulation and intact cell surface ELISA. Stimulation was done with clozapine (CLZP, 1 μM) for the indicated times. Data expressed as percent of control (here, t = 0), which is set as 100% cell-surface receptor, are mean ± S.E., and represent n = 14–15 independent replicates. *, $p < 0.01$ versus Ctl; **, $p < 0.0001$ versus Ctl by unpaired Student's *t*-test.

value of such a fragment-centered analysis is supported by a recent review on the subject of fragment-based drug design (Wasko et al., 2015). DMI and chlorpromazine have the most similar fragments attached, methylpropan-amine and dimethylpropan-amine, respectively, and their docked models indeed showed the same binding mode: both compounds occupied the center of the binding site, and their docked results overlaid well with each other, with the amine group forming a hydrogen bond with Asp$^{3.32}$ of TM3 (Fig. 8A–D). The attached fragment of clozapine is a relatively bulky methylpiperazine group. Compared to the binding modes of DMI and chlorpromazine, the docked clozapine rotated away from TM3 towards TM7, with its piperazine group forming hydrophobic interactions with Phe$^{7.39}$ of TM7 (Fig. 8E and F). Of the compounds studied, fluphenazine has the largest fragment attached. As a result, its long propylpiperazin-ethan group extended outside the ligand-binding site and formed a hydrogen bond with Glu$^{2.65}$ of TM2; its tricyclic group was pushed closer to TM5, and its trifluoromethyl group formed additional interactions with TM4 (Fig. 8G and H). These *in silico* results seem to segregate the evaluated tricyclic compounds into three distinctive modes of ligand interaction with the α_{2A}AR, consistent with the fact that three compounds exhibit distinct features in inducing endocytosis of the receptor.

As a comparison, we also docked NE. The binding site of NE is relatively small (Fig. 8I). Nonetheless, in addition to the hydrogen-bond with Asp$^{3.32}$ of TM3, the docked NE forms multiple hydrogen bonds with Ser$^{5.43}$ and Ser$^{5.42}$ of the TM5 (Fig. 8J). Hydrogen-bonding with Ser$^{5.43}$ and Ser$^{5.42}$ has been shown in agonist-bound GPCR crystal structures (Lebon et al., 2011; Warne et al., 2011; Ring et al., 2013), and is likely responsible for the activation of G protein-dependent signaling pathways. These hydrogen bonds were not observed in the docked tricyclic compounds, which likely explains their lack of G protein activation.

4. Discussion

The data presented herein provide novel insights into the molecular pharmacology of an important group of therapeutics, namely the tricyclic antipsychotics. When coupled with our extensive previously-published data on the TCAs, we can begin to paint an increasingly detailed picture of how various psychopharmacological agents belonging to the tricyclic chemical class interact with a centrally-important and psychiatric disease-relevant GPCR, namely the α_{2A}AR. As a group, all tricyclic compounds studied share the characteristic of acting as arrestin-biased ligands at the α_{2A}AR, driving Arr3 recruitment to the receptor while not stimulating any canonical heterotrimeric G protein coupling to it. However, numerous specific differences exist among the tricyclics studied in terms of the nature of Arr3 recruitment, ability to induce α_{2A}AR endocytosis, and mechanistic underpinnings of α_{2A}AR endocytosis. Furthermore, the *in silico* molecular modeling performed in the present study provides additional support for grouping the tricyclics based upon their molecular interactions with the α_{2A}AR.

Among the three antipsychotics evaluated in the present study, we have observed three different combinations of Arr3 recruitment (Fig. 3) and endocytic induction (Fig. 4). Only chlorpromazine drove both robust α_{2A}AR/Arr3 interaction and robust receptor endocytosis. This endocytic response was further shown to be fully dependent on arrestin (Fig. 5A). Clozapine was clearly less effective at driving the α_{2A}AR/Arr3 interaction, but conversely, seemed to be the most effective of the three at driving receptor endocytosis, doing so in a fully arrestin-independent fashion (Fig. 5C). Finally, fluphenazine drove robust α_{2A}AR/Arr3 interaction, on par with that driven by chlorpromazine, but failed to produce a significant endocytic response for the receptor. Given the lack of endocytosis, the functional significance of the fluphenazine-induced α_{2A}AR/Arr3 interaction remains to be elucidated; further investigation in this regard will be a goal of future work.

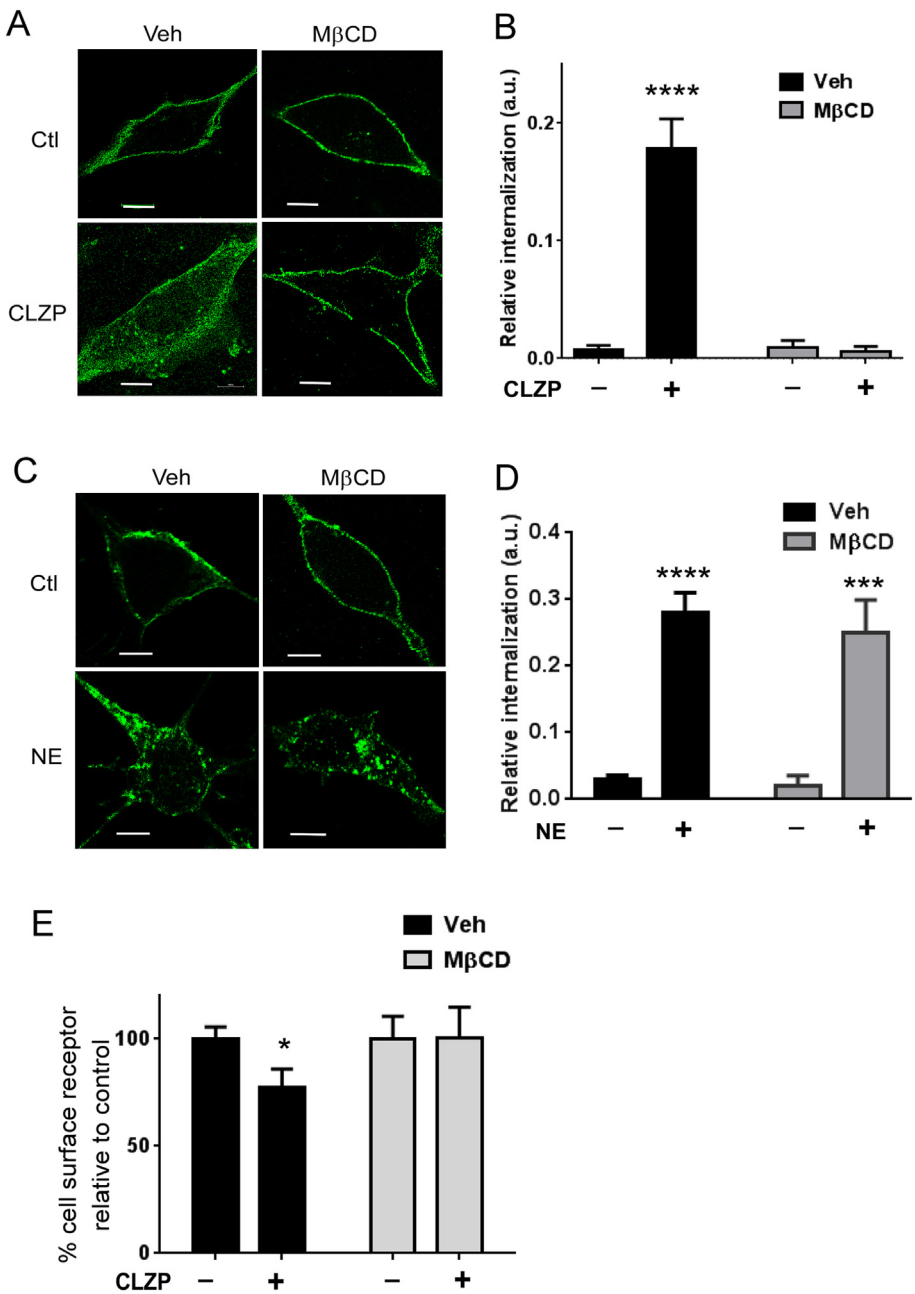

Fig. 6. Internalization of α_{2A}AR induced by clozapine, but not NE, is sensitive to disruption of lipid rafts. (A & C) Cells were pre-treated with MβCD or vehicle for 30 min and then stimulated with or without clozapine (CLZP, 1 μM, A) or NE (10 μM, C) for an additional 30 min. Cell-surface HA-α_{2A}ARs were labeled with an anti-HA antibody prior to ligand stimulation. Representative images are shown with indicated treatment. (B & D) Quantification of HA-α_{2A}AR internalization shown in A and C, respectively. 11–24 cells from at least 3 independent dishes were quantified for each condition. ***, $p < 0.001$; ****, $p < 0.0001$, versus no ligand treatment by unpaired Student's *t*-test. (E) Cells were pre-treated with MβCD or vehicle for 30 min and then stimulated with or without clozapine for an additional 5 min. Cells were then analyzed for HA-α_{2A}AR endocytosis via intact cell surface ELISA. Data are mean ± S.E. and represent n = 4–6 replicates for each condition. *, $p < 0.05$ versus no ligand treatment by unpaired Student's *t*-test.

While fluphenazine is unique among the tricyclic compounds studied thus far in not driving any appreciable α_{2A}AR endocytosis, clozapine is unique among that same group in driving robust α_{2A}AR endocytosis not mediated by the canonical arrestin-dependent machinery for GPCRs. The three TCAs which we have previously studied (Cottingham et al., 2011, 2014) and chlorpromazine all drive α_{2A}AR endocytosis in an arrestin-mediated fashion. Clozapine-induced α_{2A}AR endocytosis also seems to occur independent of clathrin-coated pits (Fig. 5C), which mediate the predominantly-engaged pathway for GPCR endocytosis (Hanyaloglu and von Zastrow, 2008). Instead, a manipulation known to disrupt the lipid rafts completely abolished clozapine-induced internalization (Fig. 6A, B and 6E). In addition, following clozapine exposure, internalized α_{2A}ARs were found to colocalize with caveolin-1 within the cytoplasm (Fig. 7A and B). These findings indicate that clozapine induces endocytosis through machinery relying on caveolae and lipid rafts. It is worth noting that there is a significant proportion of α_{2A}ARs colocalized with caveolin-1 in the naïve state (Fig. 7A and B). It is therefore conceivable that clozapine specifically engages this pool of receptors in the lipid rafts and causes their

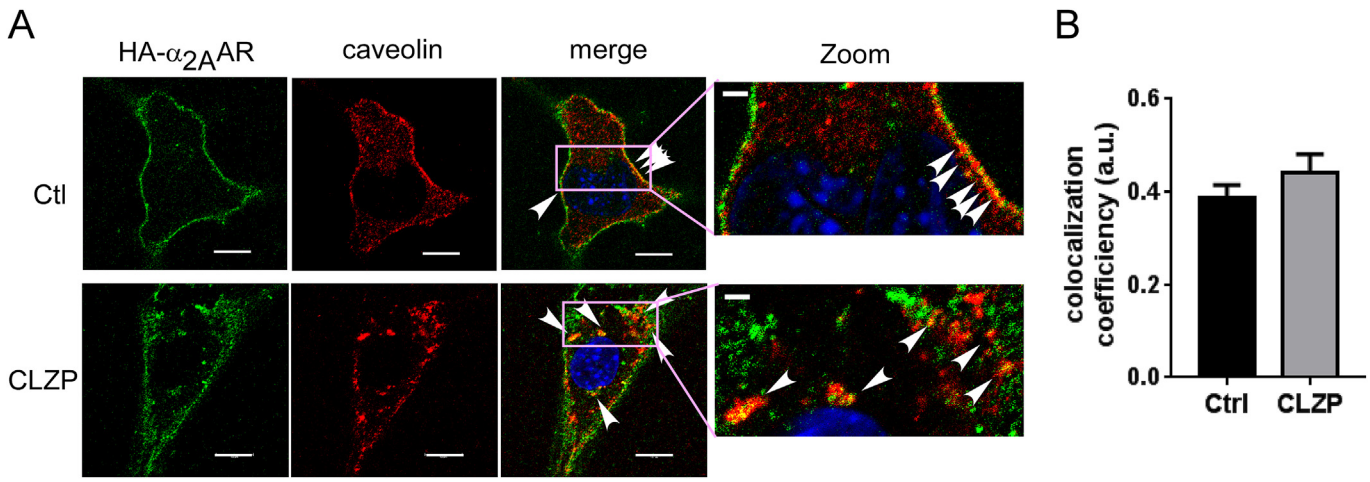

Fig. 7. α_{2A}ARs are partially localized in caveolin-1 positive intracellular compartments following clozapine treatment. (A) Co-immunostaining of HA-α_{2A}AR and caveolin-1 in cells treated with or without clozapine. Cell-surface HA-α_{2A}AR was labeled with an HA antibody prior to clozapine stimulation. Arrow heads indicate colocalization between HA-α_{2A}AR and caveolin-1. (B) Quantification of colocalization coefficiency between HA-α_{2A}AR and caveolin-1. 12–16 cells from at least 3 independent dishes were quantified for each condition.

internalization.

The receptor internalization driven by tricyclic compounds has the potential to play an important physiological role. *In vivo*, this tricyclic-induced internalization would not occur in a vacuum; rather, it would occur within the context of complex, multifactorial synapses within the CNS. Most CNS synapses, particular those of the cortical regions associated with the sophisticated cognitive processes modulated by antipsychotics, comprise multiple presynaptic terminals releasing multiple neurotransmitters, which in turn act via multiple receptors (Molinoff, 2011). The functioning of such synapses is determined by a dynamic balance of numerous neurotransmitter/receptor interactions. Therefore, any pharmacological intervention which alters that balance has the potential to, in turn, alter synaptic function. Our data clearly establish that potential for clozapine and chlorpromazine, in the form of their ability to alter cell-surface availability of α_{2A}ARs by driving their internalization. Further study will obviously be required to elucidate precise effects on the relevant synapses, but it has become increasingly apparent that endocytosis of neurotransmitter receptors can have numerous functional ramifications by altering the plasma membrane localization of receptors, directing receptors into intracellular sorting pathways, and allowing for receptor-initiated signaling from endosomes (von Zastrow and Williams, 2012; Irannejad et al., 2015).

It seems clear that, at least with respect to Arr3-recruiting and endocytic profiles when acting as direct α_{2A}AR ligands, the various tricyclic compounds studied to-date can be organized into three different functional groups. The first group is the most populous, comprising all three TCAs (DMI, imipramine, and amitriptyline) plus the antipsychotic chlorpromazine, and displays a profile of driving Arr3 recruitment to the α_{2A}AR, followed by rapid arrestin-dependent α_{2A}AR endocytosis. The second group has but a single member, the antipsychotic clozapine, and displays a profile of weakly driving Arr3 recruitment to the receptor while simultaneously driving rapid arrestin- and clathrin-independent receptor endocytosis. The third group also has but a single member, the antipsychotic fluphenazine, and displays a profile of driving robust Arr3 recruitment to the receptor with no detectable receptor endocytosis.

Our *in silico* modeling analysis provides structural insights into how the tricyclic ligands interact with the extracellular face of an α_{2A}AR homology model, and supports the existence of the same three different sub-groups of tricyclics. While the docked NE forms multiple hydrogen bonds with Ser$^{5.43}$ and Ser$^{5.42}$ of the TM5 (Fig. 8J), which are important for G protein activation, none of the tricyclic compounds do so (Fig. 8B, D, F and H), corresponding nicely with their inability to activate heterotrimeric G proteins. Among the tricyclics, the docked models of the TCA DMI and chlorpromazine showed good overlap with each other, suggesting that they interact similarly with the α_{2A}AR ligand-binding pocket (Fig. 8A–D); this correlates with their nearly identical Arr3-recruiting and endocytic profiles. Perhaps unsurprisingly, of the selected antipsychotics, chlorpromazine is the most structurally similar to DMI; it should be noted that the other two previously-studied TCAs also share extremely similar characteristic long side chains (Cottingham et al., 2014). By contrast, the docked models of clozapine (Fig. 8E and F) and fluphenazine (Fig. 8G and H) suggest molecular interactions with the α_{2A}AR distinct both from each other and from the TCA/chlorpromazine group. In terms of its ability to drive α_{2A}AR endocytosis and its *in silico* interaction with the receptor, fluphenazine stands alone: it is the only tricyclic compound studied that does not drive α_{2A}AR endocytosis, and that displays a molecular ligand/receptor interaction extending outside of the classic ligand-binding site.

Given recent and ever-expanding advances in GPCR structural determination and modeling capability (Kobilka, 2011; Shoichet and Kobilka, 2012; Costanzi, 2014), and the great potential of fragment-based drug design for central nervous system targets (Wasko et al., 2015), we believe our data are of great potential significance to the field. It is, of course, extremely important to note that future studies will be required to definitively establish a causal link between the varying *in silico* molecular interactions and the functional differences seen in a real biological system. Nevertheless, our present body of work at least establishes a clear correlation between the two that is very much worth following up on, and could have practical ramifications for future drug design.

Funding

This work was supported by the National Institute of Mental Health (Grant MH081917, to QW), the Brain & Behavior Research Foundation (Independent Investigator Award to QW) and by grants

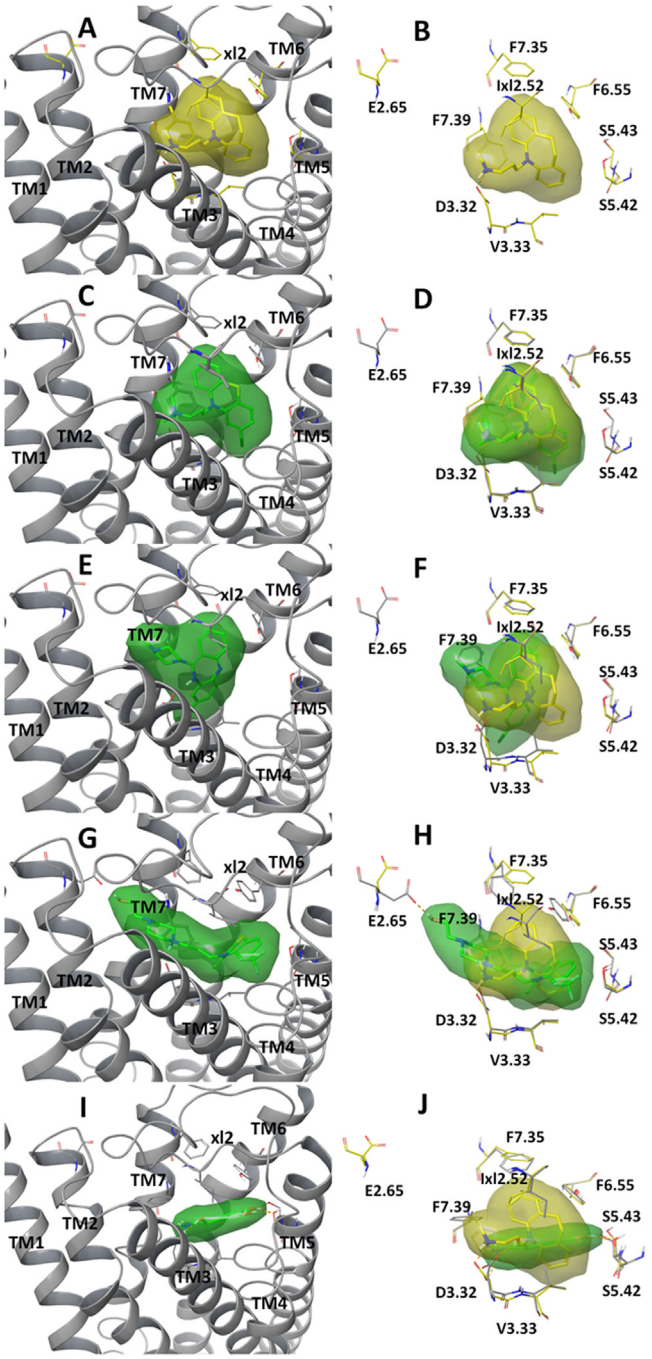

Fig. 8. Structural presentation of the predicted binding modes of tricyclic compounds desipramine (A, B), chlorpromazine (C, D), clozapine (E, F), fluphenazine (G, H) and norepinephrine (I and J) to α_{2A}AR. Each compound was shown in solid sticks buried in transparent molecular surface colored in yellow (desipramine) or green (chlorpromazine, clozapine, fluphenazine and norepinephrine). The left panel (A, C, E, G, I) illustrated the binding modes with the receptor shown in ribbons. The right panel (B, D, F, H, J) compared the binding modes by overlapping with docked desipramine with key binding site residues explicitly shown in yellow-colored (desipramine-docked model) or grey-colored (chlorpromazine, clozapine and fluphenazine docked models) carbon atoms. Hydrogen-bonds were shown in dashed purple lines. Residue numbers were based on Ballesteros Weinstein sequencing.

(to CC) from the Kentucky Biomedical Research Infrastructure Network, an Institutional Development Award (IDeA) program funded by the National Institute of General Medical Sciences (Grant P20GM103436).

Acknowledgments

Our thanks to the UAB High Resolution Imaging Facility for assistance with FLIM-FRET and to Dr. Robert J. Lefkowitz (Duke University) for generously providing the Arr2,3$^{-/-}$ MEF cell line.

Abbreviations

AR	adrenergic receptor
Arr	arrestin
CFP	cyan fluorescent protein
DMI	desipramine
ELISA	enzyme-linked immunosorbent assay
FLIM	fluorescence lifetime imaging microscopy
FRET	fluorescence resonance energy transfer
GPCR	G protein-coupled receptor
HCl	hydrochloride
Gpp(NH)p	5′-guanylimidodiphosphate
GTPγS	guanosine 5′-*O*-(thio)triphosphate
MEF	mouse embryonic fibroblast
NE	norepinephrine
YFP	yellow fluorescent protein

References

Allen, J.A., Halverson-Tamboli, R.A., Rasenick, M.M., 2007. Lipid raft microdomains and neurotransmitter signalling. Nat. Rev. Neurosci. 8, 128–140.
Baldessarini, R.J., 2006. Drug therapy of depression and anxiety disorders. In: Brunton, L., et al. (Eds.), Goodman & Gilman's the Pharmacological Basis of Therapeutics. McGraw-Hill, Inc., New York, pp. 429–460.
Baldessarini, R.J., Tarazi, F.I., 2006. Pharmacotherapy of psychosis and mania. In: Brunton, L., et al. (Eds.), Goodman & Gilman's the Pharmacological Basis of Therapeutics. McGraw-Hill, Inc., New York.
Ballesteros, J.A., Weinstein, H., 1995. Integrated methods for the construction of three-dimensional models and computational probing of structure-function relations in G protein-coupled receptors. Methods Neurosci. 25, 366–428.
Barnett-Norris, J., Lynch, D., Reggio, P.H., 2005. Lipids, lipid rafts and caveolae: their importance for GPCR signaling and their centrality to the endocannabinoid system. Life Sci. 77, 1625–1639.
Brady, A.E., Wang, Q., Allen, P.B., Rizzo, M., Greengard, P., Limbird, L.E., 2005. Alpha 2-adrenergic agonist enrichment of spinophilin at the cell surface involves beta gamma subunits of Gi proteins and is preferentially induced by the alpha 2A-subtype. Mol. Pharmacol. 67, 1690–1696.
Brady, A.E., Wang, Q., Colbran, R.J., Allen, P.B., Greengard, P., Limbird, L.E., 2003. Spinophilin stabilizes cell surface expression of alpha 2B-adrenergic receptors. J. Biol. Chem. 278, 32405–32412.
Chen, Y., Liu, Y., Cottingham, C., McMahon, L., Jiao, K., Greengard, P., Wang, Q., 2012. Neurabin scaffolding of adenosine receptor and RGS4 regulates anti-seizure effect of endogenous adenosine. J. Neurosci. Off. J. Soc. Neurosci. 32, 2683–2695.
Cheng, Y., Prusoff, W.H., 1973. Relationship between the inhibition constant (K1) and the concentration of inhibitor which causes 50 per cent inhibition (I50) of an enzymatic reaction. Biochem. Pharmacol. 22, 3099–3108.
Chini, B., Parenti, M., 2004. G-protein coupled receptors in lipid rafts and caveolae: how, when and why do they go there? J. Mol. Endocrinol. 32, 325–338.
Chou, T., 1974. Relationships between inhibition constants and fractional inhibition in enzyme-catalyzed reactions with different numbers of reactants, different reaction mechanisms, and different types and mechanisms of inhibition. Mol. Pharmacol. 10, 235–247.
Costanzi, S., 2014. Modeling G protein-coupled receptors in complex with biased agonists. Trends Pharmacol. Sci. 35, 277–283.
Cottingham, C., Chen, Y., Jiao, K., Wang, Q., 2011. The antidepressant desipramine is an arrestin-biased ligand at the alpha(2A)-adrenergic receptor driving receptor down-regulation in vitro and in vivo. J. Biol. Chem. 286, 36063–36075 (PMID 21859713).
Cottingham, C., Jones, A., Wang, Q., 2012a. Desipramine selectively potentiates norepinephrine-elicited ERK1/2 activation through the alpha2A adrenergic receptor. Biochem. Biophys. Res. Commun. 420, 161–165 (PMID 22405824).
Cottingham, C., Li, X., Wang, Q., 2012b. Noradrenergic antidepressant responses to desipramine in vivo are reciprocally regulated by arrestin3 and spinophilin. Neuropharmacology 62, 2354–2362 (PMID 22405824).
Cottingham, C., Percival, S., Birky, T., Wang, Q., 2014. Tricyclic antidepressants exhibit variable pharmacological profiles at the α2A adrenergic receptor. Biochem. Biophys. Res. Commun. 451, 461–466 (PMID 25128275).
Cottingham, C., Wang, Q., 2012. α2 adrenergic receptor dysregulation in depressive disorders: implications for the neurobiology of depression and antidepressant therapy. Neurosci. Biobehav Rev. 36, 2214–2225.

De Vos, H., Vauquelin, G., De, K.J., De Backer, J.P., Van, L.I., 1992. Regional distribution of alpha 2A- and alpha 2B-adrenoceptor subtypes in postmortem human brain. JNeurochem 58, 1555–1560.
Glide, Version 6.3, 2014. Schrodinger, LLC, New York, NY.
Hansen, S.H., Sandvig, K., van Deurs, B., 1993. Clathrin and HA2 adaptors: effects of potassium depletion, hypertonic medium, and cytosol acidification. J. Cell Biol. 121, 61–72.
Hanyaloglu, A.C., von Zastrow, M., 2008. Regulation of GPCRs by endocytic membrane trafficking and its potential implications. Annu. Rev. Pharmacol. Toxicol. 48, 537–568.
Irannejad, R., Tsvetanova, N.G., Lobingier, B.T., von Zastrow, M., 2015. Effects of endocytosis on receptor-mediated signaling. Curr. Opin. Cell Biol. 35, 137–143.
Kobilka, B.K., 2011. Structural insights into adrenergic receptor function and pharmacology. Trends Pharmacol. Sci. 32, 213–218.
Lebon, G., Warne, T., Edwards, P.C., Bennett, K., Langmead, C.J., Leslie, A.G.W., Tate, C.G., 2011. Agonist-bound adenosine A2A receptor structures reveal common features of GPCR activation. Nature 474, 521–525.
LigPrep, Version 2.3, 2009. Schrodinger, LLC, New York, NY.
Limbird, L.E., 2005. Cell Surface Receptors: a Short Course on Theory and Methods, third ed. Springer Science + Business Media, Inc., New York.
Lu, R., Li, Y., Zhang, Y., Chen, Y., Shields, A.D., Winder, D.G., Angelotti, T., Jiao, K., Limbird, L.E., Zhou, Y., Wang, Q., 2009. Epitope-tagged receptor knock-in mice reveal that differential desensitization of alpha2-adrenergic responses is because of ligand-selective internalization. J. Biol. Chem. 284, 13233–13243.
MacMillan, L.B., Hein, L., Smith, M.S., Piascik, M.T., Limbird, L.E., 1996. Central hypotensive effects of the alpha2a-adrenergic receptor subtype. Science 273, 801–803.
Meyer, J.M., 2011. Pharmacotherapy of psychosis and mania. In: Brunton, L., et al. (Eds.), Goodman & Gilman's the Pharmacological Basis of Therapeutics. McGraw-Hill Medical.
Molinoff, P.B., 2011. Neurotransmission and the central nervous system. In: Brunton, L.L. (Ed.), Goodman & Gilman's the Pharmacological Basis of Therapeutics, Online Edition. The McGraw-Hill Companies, Inc.
Prime, Version 1.6, 2007. Schrodinger, LLC, New York, NY.
Rajagopal, S., Rajagopal, K., Lefkowitz, R.J., 2010. Teaching old receptors new tricks: biasing seven-transmembrane receptors. Nat. Rev. Drug Discov. 9, 373–386.
Ring, A.M., Manglik, A., Kruse, A.C., Enos, M.D., Weis, W.I., Garcia, K.C., Kobilka, B.K., 2013. Adrenaline-activated structure of β2-adrenoceptor stabilized by an engineered nanobody. Nature 502, 575–579.
Sastre, M., García-Sevilla, J.A., 1994. Alpha 2-adrenoceptor subtypes identified by [3H]RX821002 binding in the human brain: the agonist guanoxabenz does not discriminate different forms of the predominant alpha 2A subtype. J. Neurochem. 63, 1077–1085.
Schramm, N.L., Limbird, L.E., 1999. Stimulation of mitogen-activated protein kinase by G protein-coupled alpha(2)-adrenergic receptors does not require agonist-elicited endocytosis. J. Biol. Chem. 274, 24935–24940.
Sherman, W., Day, T., Jacobson, M.P., Friesner, R.A., Farid, R., 2006. Novel procedure for modeling ligand/receptor induced fit effects. J. Med. Chem. 49, 534–553.
Shoichet, B.K., Kobilka, B.K., 2012. Structure-based drug screening for G-protein-coupled receptors. Trends Pharmacol. Sci. 33, 268–272 (PMID 22503476).
Tan, C.M., Brady, A.E., Nickols, H.H., Wang, Q., Limbird, L.E., 2004. Membrane trafficking of G protein-coupled receptors. Annu. Rev. Pharmacol. Toxicol. 44, 559–609.
Tan, C.M., Wilson, M.H., MacMillan, L.B., Kobilka, B.K., Limbird, L.E., 2002. Heterozygous alpha 2A-adrenergic receptor mice unveil unique therapeutic benefits of partial agonists. Proc. Natl. Acad. Sci. U. S. A. 99, 12471–12476.
Violin, J.D., Lefkowitz, R.J., 2007. Beta-arrestin-biased ligands at seven-transmembrane receptors. Trends Pharmacol. Sci. 28, 416–422.
von Zastrow, M., Williams, J.T., 2012. Modulating neuromodulation by receptor membrane traffic in the endocytic pathway. Neuron 76, 22–32.
Wang, Q., Lu, R., Zhao, J., Limbird, L.E., 2006. Arrestin serves as a molecular switch, linking endogenous alpha2-adrenergic receptor to SRC-dependent, but not SRC-independent, ERK activation. J. Biol. Chem. 281, 25948–25955.
Wang, Q., Zhao, J., Brady, A.E., Feng, J., Allen, P.B., Lefkowitz, R.J., Greengard, P., Limbird, L.E., 2004. Spinophilin blocks arrestin actions in vitro and in vivo at G protein-coupled receptors. Science 304, 1940–1944.
Wang, R., Macmillan, L.B., Fremeau Jr., R.T., Magnuson, M.A., Lindner, J., Limbird, L.E., 1996. Expression of alpha 2-adrenergic receptor subtypes in the mouse brain: evaluation of spatial and temporal information imparted by 3 kb of 5' regulatory sequence for the alpha 2A AR-receptor gene in transgenic animals. Neuroscience 74, 199–218.
Warne, T., Moukhametzianov, R., Baker, J.G., Nehmé, R., Edwards, P.C., Leslie, A.G.W., Schertler, G.F.X., Tate, C.G., 2011. The structural basis for agonist and partial agonist action on a β(1)-adrenergic receptor. Nature 469, 241–244.
Wasko, M.J., Pellegrene, K.A., Madura, J.D., Surratt, C.K., 2015. A role for fragment-based drug design in developing novel lead compounds for central nervous system targets. Front. Neurol. 6.
Xu, J., Chen, Y., Lu, R., Cottingham, C., Jiao, K., Wang, Q., 2008. Protein kinase A phosphorylation of spinophilin modulates its interaction with the alpha 2A-adrenergic receptor (AR) and alters temporal properties of alpha 2AAR internalization. J. Biol. Chem. 283, 14516–14523.